Supplementary Information: Experimental Diffusiophoresis of Porous and Non-Porous Silica Particles in Dead-End Pore Microchannel Geometry

Mansoureh Rashidi, Matina Nooryani, Giovanniantonio Natale, Anne M. Benneker

May 1, 2026

Appendix A: Hydrodynamic Drag Force Measurement

To compare the hydrodynamic drag force exerted on porous and non-porous particles, an optical tweezers instrument (Tweez 305, Aresis) was used. The study involved 2 μm non-porous silica particles and two types of 2 μm porous silica particles (SOLADTM particles, Glantreo) with pore sizes of 2 nm (BET surface area = 1221.7322 $\frac{\mathrm{m}^2}{\mathrm{g}}$) and 100 nm (BET surface area = 24.711 $\frac{\mathrm{m}^2}{\mathrm{g}}$). The particles were suspended in DI water using a bath sonicator in a very dilute regime (¡ 10^{-5} volume fraction). To measure the drag force exerted on different types of particles, constant velocities in the range of 0-20 $\frac{\mu\mathrm{m}}{\mathrm{s}}$ were applied.

Figure 1 shows the measured drag force exerted on the porous and non-porous particles. The obtained forces for non-porous particle are fitted with the Stokes' drag equation (presented in eq.1) [1], and for porous particles fitted with the equation presented by Neale et al. in eq.2[2] in which, η is the viscosity of DI water at $21 \pm 1°\mathrm{C}$ ($0.00095\frac{\mathrm{kg}}{\mathrm{m.s}}$), a is the particle radius (m), V is the exerted velocity ($\frac{\mathrm{m}}{\mathrm{s}}$) and Ω is the drag coefficient for porous particles defined in eq.3. In this equation, Γ is the dimensionless permeability defined as $\Gamma = \frac{a}{\sqrt{k}}$, and k is the permeability of porous particles (m^2) [2].

$$F = 6\pi\eta a V \tag{1}$$

$$F = 6\pi\eta a \Omega V \tag{2}$$

$$\Omega = \frac{2\Gamma^2(1 - \frac{\tanh\Gamma}{\Gamma})}{2\Gamma^2 + 3(1 - \frac{\tanh\Gamma}{\Gamma})} \tag{3}$$

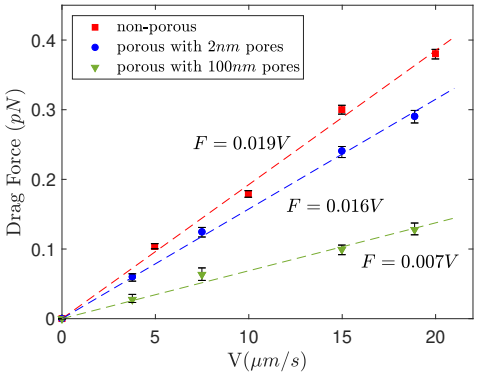

Figure 1: Experimental drag force exerted on 2 μm non-porous silica particles and 2 μm porous silica particles with 2 and 100 nm pore sizes. Linear fits represent the theoretical drag force exerted on the particles using eqs.1 and 2

For non-porous particles, the experimental slope obtained from the fitted line ($0.019\frac{\text{mg}}{\text{s}}$) shows good agreement with the theoretical slope ($\frac{F}{V} = 0.018\frac{\text{mg}}{\text{s}}$) derived from equations 1, with a relative error of about 5%. It is observed that the hydrodynamic drag force exerted on porous particles is smaller than that on non-porous particles because, in porous particles, fluid flow occurs both around and through the particle [3]. Figure 1 also shows that the drag force decreases significantly with increasing pore size from 2 nm to 100 nm. The drag force on particles with larger pores (100 nm) is 50% less than that on small-pore particles and approximately 65% less than that on non-porous particles.

Using the experimental slopes obtained from Figure 1 and eqs. 2 and 3, the permeability of porous particles with 2 and 100 nm pore sizes can be determined as 9.68×10^{-3} and $3.07 \times 10^{-1}(\mu\text{m})^2$, respectively. This shows that porous particles with 100 nm pore size have higher permeability compared to those with smaller pores. Therefore, flow can penetrate more easily into porous particles with 100 nm pores, reducing drag. The ratio of pore size to water molecule size (2.75 Å) [4] affects the fluid permeability through the porous particles' interior. In our experiment, as the ratio of pore size to water molecule size increases from 7.27 to 363.6, the drag force reduces by 50%, as shown in Figure 1. This indicates that the ratio of the particle's pore size to the solute molecule size is a key parameter affecting permeability and overall hydrodynamic drag force. For particles with 2 nm pores, this ratio is 7.27, leading to an 18% reduction in drag force compared to non-porous particles.

Appendix B: Calculated Velocity Ratio $\frac{U^{(c)}}{U^{(e)}}$ for NaOH and NaCl Cases

Tables 1 and 2 present the calculated velocity ratios of chemiphoretic (CP) to electrophoretic (EP) velocities, reflecting the relative contributions of each mechanism to particle motion under concentration gradients of NaOH and NaCl, respectively. These ratios help evaluate whether CP or EP is the dominant driving force in each electrolyte system.

Table 1: Calculated velocity ratio $\frac{U^{(c)}}{U^{(e)}}$ for non-porous particles and porous particles with 2 nm and 10 nm pore sizes under the transient NaOH concentration gradient. The experiment captures particle behavior across the pH range of 7 to 12.

	$\frac{U^{(c)}}{U^{(e)}}$non − porous	$\frac{U^{(c)}}{U^{(e)}}$porous (2nm)	$\frac{U^{(c)}}{U^{(e)}}$porous (10nm)
***p*H=7**	–	–	–
***p*H=8**	0.4667	0.3585	0.3357
***p*H=9**	0.5914	0.3403	0.3479
***p*H=10**	0.4939	0.3181	0.3403
***p*H=11**	0.6027	0.3111	0.3165
***p*H=12**	0.4237	0.3388	0.3848

Empty cells in this table correspond to pH conditions where the key assumption ($\lambda, \mathrm{e}^{\frac{1}{2}|\bar{\zeta}|} \leq 1$) is violated, making the velocity ratio calculations unreliable. In particular, for porous particles that migrate toward regions of lower electrolyte concentration (toward the main channel), the resulting highly diluted NaOH conditions lead to a significantly thickened EDL. This large EDL thickness invalidates the other assumption required for applying eqs. 5 and 6 in the text, making the velocity ratios inapplicable under these conditions.

Table 2: Calculated velocity ratio $\frac{U^{(c)}}{U^{(e)}}$ for non-porous particles and porous particles with 2 nm and 10 nm pore sizes under the transient NaCl concentration gradient based on the initial NaCl concentration.

	$\frac{U^{(c)}}{U^{(e)}}$non − porous	$\frac{U^{(c)}}{U^{(e)}}$porous (2nm)	$\frac{U^{(c)}}{U^{(e)}}$porous (10nm)
10 mM	0.6819	0.5800	0.3830

Appendix C: *p*H Variation in the Dead-End Pore and its Effect on the Particles DP Velocity

A numerical model was developed to predict the *p*H variation in the dead-end pore and its effect on the DP velocity of particles using the Nernst-Planck equation relating the concentration of the *i*-th ion to its flux in the x-direction (see Figure 1) as shown in eqs.4 and 5 [5, 6].

$$\frac{\partial C_i}{\partial t} = \frac{\partial j_i}{\partial x} \tag{4}$$

$$J_i = -D_i\left(\frac{\partial C_i}{\partial x} - \frac{z_i e}{k_B T} C_i \frac{\partial \psi}{\partial x}\right) \tag{5}$$

In this equation, j_i and D_i are the flux and diffusion coefficient of the i-th ion of the electrolyte, and ψ is the electric potential generated by the ion migration in the system. In this model, we assume that the solution is electrically neutral and that the net electric current is zero. These conditions can be expressed by the following equations:

$$\Sigma\ Z_i C_i = 0 \tag{6}$$

$$\Sigma\ Z_i j_i = 0 \tag{7}$$

Combining eqs.5 and 7 yields eq.8 to describe the gradient of electrical potential:

$$\frac{\partial \psi}{\partial x} = \frac{\Sigma_i D_i Z_i \frac{\partial C_i}{\partial x}}{\Sigma_i D_i Z_i^2 C_i} \tag{8}$$

As the solution in the dead-end pore is gradually replaced by DI water, the *p*H changes over time, which in turn affects the ζ-potential of the particles. To relate the ζ-potential to the *p*H, a linear relationship, expressed in eq.9, is used in this model [5].

$$\zeta(pH) = -\frac{\Delta\zeta}{\Delta pH}(pH - pH_{solution}) + \zeta_{solution} \tag{9}$$

In this equation, pH_{solution} and ζ_{solution} represent the pH and ζ-potential of the solution inside the dead-end pore, whose properties vary over time. In addition, $\Delta\zeta = |\zeta_{\text{solution}} - \zeta_{\text{DIwater}}|$ and $\Delta pH = pH_{\text{solution}} - pH_{\text{DIwater}}$. By solving eq. 5 to obtain $C_i(x)$, DP velocity of the particle can be evaluated by [7, 8]:

$$U = \frac{\epsilon}{\mu}\left(\frac{\partial \psi}{\partial x}\zeta(pH) + \frac{\partial \ln I}{\partial x}\frac{\zeta^2(pH)}{8}\right) \tag{10}$$

In eq. 10, $I = \frac{1}{2}\sum_i Z_i^2 C_i$ represents the ionic strength of the electrolyte. Figure 2.A illustrates the variation of the pH in the dead-end pore for the HCl case along the length of the pore at different time steps. The corresponding ζ-potential of the particles for all particle types is shown in Figure 3. It can be observed that within the corresponding pH range in this case, the sign of the ζ-potential remains unchanged.

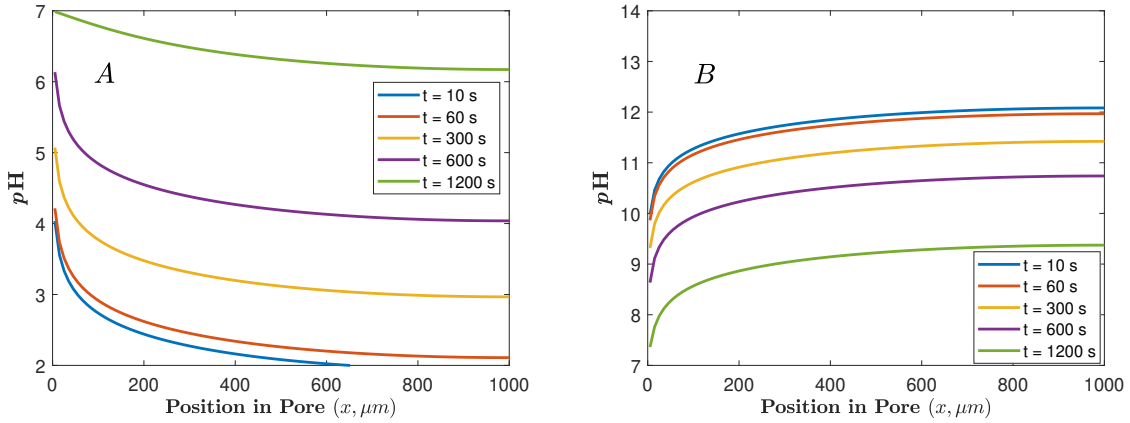

Figure 2: Variation of the pH of the solution in the dead-end pore along the pore length under a transient A) HCl concentration gradient, and B) NaOH concentration gradient as a function of time. In these plots, $x = 0$ represents the entrance of the dead-end pore, while $x = 1000\,\mu$m corresponds to the end of the pore.

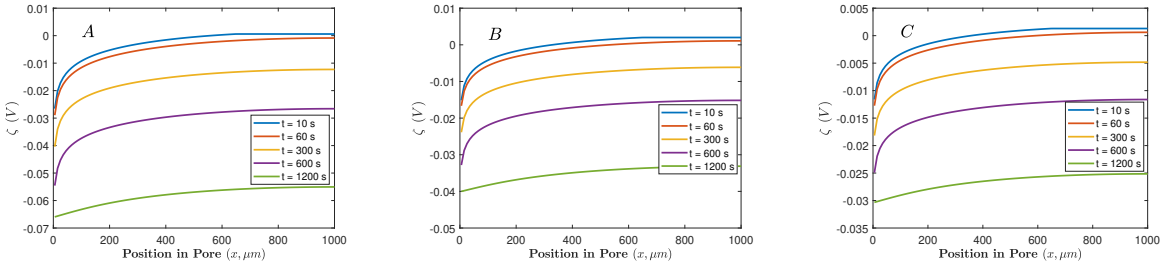

Figure 3: Variation of the ζ-potential of the particles in the dead-end pore along the pore length under a transient HCl concentration gradient as a function of time for A) non-porous particles, B) porous particles with a 2 nm pore size, and C) porous particles with a 10 nm pore size.

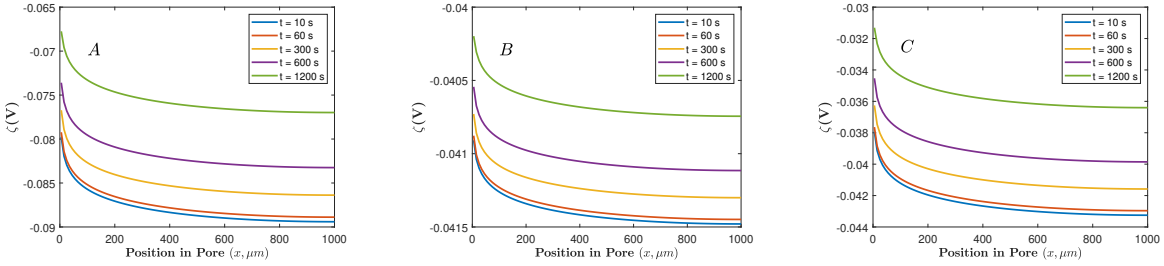

Figure 4: Variation of the ζ-potential of the particles in the dead-end pore along the pore length under a transient NaOH concentration gradient as a function of time for A) non-porous particles, B) porous particles with a 2 nm pore size, and C) porous particles with a 10 nm pore size.

Figures 4 and 5 show the variation of the ζ-potential and the DP velocity of the particles along the pore length for the NaOH case, considering non-porous particles and two types of porous particles, as a function of time. As can be observed, the numerical simulation predicts that all particle types move toward the region of higher electrolyte concentration. However, this behavior agrees with the experimental observations only for the non-porous particles. The discrepancy for porous particles could be attributed to their internal structure and to the competition between EP and CP, possibly

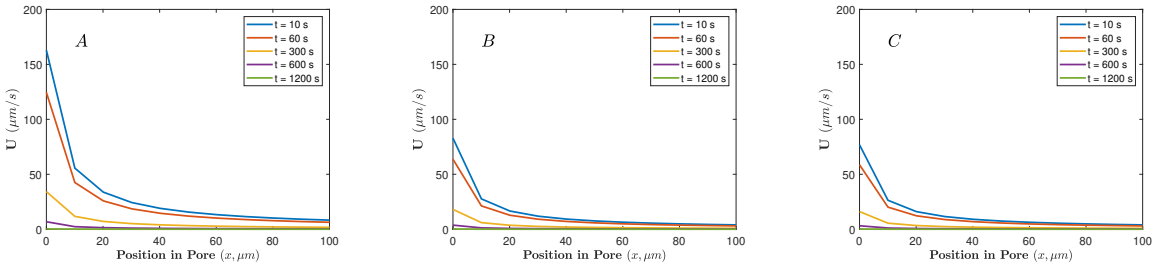

Figure 5: Simulated DP velocity of particles in the microchannel over a 100 μm segment of the dead-end pore geometry under a transient concentration gradient of NaOH as a function of time for A) Non-porous particles, B) porous particles with 2 nm pore size, C) porous particles with 10 nm pore size.

influenced by the presence of DLP type II, as explained in the text, which affects the DP velocity of porous particles.

In addition, these Figures indicate that the sign of the ζ-potential remains constant within the studied pH range $(7-12)$. Therefore, the pH variation does not alter the direction of particle motion.

References

[1] G. G. Stokes *et al.*, 1851.

[2] G. Neale, N. Epstein and W. Nader, *Chemical Engineering Science*, 1973, **28**, 1865–1874.

[3] R. Wu and D. Lee, *Chemical Engineering Science*, 1998, **53**, 3571–3578.

[4] D. Hankins, J. Moskowitz and F. Stillinger, *The Journal of Chemical Physics*, 1970, **53**, 4544–4554.

[5] E. Coleman and A. Gupta, *Physical Review Fluids*, 2025, **10**, 103701.

[6] B. M. Alessio, S. Shim, E. Mintah, A. Gupta and H. A. Stone, *Physical Review Fluids*, 2021, **6**, 054201.

[7] T.-Y. Chiang and D. Velegol, *Journal of colloid and interface science*, 2014, **424**, 120–123.

[8] A. Gupta, B. Rallabandi and H. A. Stone, *Physical Review Fluids*, 2019, **4**, 043702.